Mechanical analog of temperature for the description of force distribution in static granular packings

A. H. W. Ngan
Department of Mechanical Engineering, The University of Hong Kong, Pokfulam Road, Hong Kong, People's Republic of China
(Received 7 October 2002; revised manuscript received 2 January 2003; published 11 July 2003)

It is shown that in a stressed granular packing, the effect of the applied pressure and structural randomness on the contact force distribution can be described accurately by a variational principle of minimizing energy subject to the constraint of keeping entropy at a fixed value. The constraint on entropy may be regarded as a measure of the degree of retained disorderness in the system. This procedure leads to the introduction of a parameter known as the ''mechanical temperature.'' Similar to the role of the conventional thermal temperature in a thermal system, the mechanical temperature can be viewed as a parameter controlling the mixity between energy minimization and entropy maximization in the equilibrium condition.

DOI: 10.1103/PhysRevE.68.011301 PACS number(s): 45.05.+x, 45.70.−n, 81.05.Rm, 05.70.−a

I. INTRODUCTION

Either by design or otherwise, many engineering materials are randomly structured. Examples include atomistically disordered or partially disordered materials, such as amorphous solids or polymers, and macroscopically disordered materials, such as foam materials or random grain piles. Because of structural randomness, the internal force distribution in these materials due to external loadings would not be uniform. Earlier experiments and computer simulations have concluded that intergranular contact forces in a granular packing under gravity or compaction loading, in general, follow an exponential probabilistic distribution, in which large forces are exponentially rare [1–3]. More recent experiments have focused on the force distribution at large applied loads so that the particles enter the deformable regime. Some authors have concluded that the force distribution observed transits into a Gaussian form in the deformable regime [4,5]. Others have found distributions that are peaked at about the mean force, but the large force regime still follows an exponential tail with an increasing slope as the load increases [6]. From computer simulations, O'Hern *et al.* [7,8] have also found Gaussian force distributions in frictionless granular packings, as well as in supercooled liquids and foams as temperature decreases.

Much of the theoretical understanding of the exponential probabilistic distribution and the diffusive nature of the contact forces in grain piles available to date is provided by the ''q model'' [9] or its variants [10–15]. The q model, originally developed to understand random river networks, is based on the assumption of a hierarchy structure in which force (as in the case of uniaxial compaction loading) or body weight (as in the case of loading due to gravity) disperses through the material volume from one end to another. The q model is successful in providing a mean-field description of how forces percolate throughout the granular medium, but it is self-inconsistent in the sense that a regular structure is required for analyticity but force transmission amongst grains is assumed to be random. Also, the q model predicts power-law distribution at small forces, implying vanishing probability distribution at zero force—a prediction that disagrees with experimental findings [16].

A number of authors have also investigated the applicability of statistical physics concepts in describing granular systems. In modeling avalanches on the slopes of a flowing sandpile, Jaeger, Liu, and Nagel mimic the effects of mechanical vibrations by an effective temperature [17]. Edwards [18] has studied extensively the application of entropy concepts to the description of configurations of random grain piles. Edwards' theory is aimed at describing how space is filled by the granular volumes, taking into account randomness as expressed by an entropy function. He transformed the laws of thermodynamics into the granular analogies by drawing parallelism between energy and volume, and the incorporation of the entropy function introduces an analog of temperature, which he called the ''compactivity.'' The extension of Edwards' entropy and compactivity to describe contact forces, however, has not been pursued. Bagi [19] and Evesque [20], on the other hand, have argued that the principle of maximum entropy should be applicable to describe force distribution in random granular packings. However, the prediction of the maximum entropy assumption is the exponential Maxwell-Boltzmann (MB) distribution, which is not in agreement with the Gaussian distribution mentioned above. Recently, Ono *et al.* [21] investigated five possible definitions of an effective temperature to describe the fluctuations of elastic bubbles during viscous shear. Their results indicate that an athermal elastic foam during shear can be described by statistical mechanics with an effective temperature that depends on the shear rate.

This work is an attempt to develop further the application of statistical mechanics concepts in the description of random granular materials as advocated in the previous studies outlined above [18–21]. We first argue that the degree of retained randomness in a jammed structure can be represented by an entropy functional. We then predict equilibrium by minimizing the strain energy of the system, subject to the constraint imposed by the retained entropy. The result is a transition from the exponential to Gaussian form of the force distribution, as the retained entropy decreases. To verify the results, computer simulations using the discrete element method were also carried out. It is expected that the concepts developed in this work should also be applicable to other random materials such as open cell foam materials.

II. THEORY

A. Entropy as a measure of retained disorderness

The global ground state of a granular packing under loading should evidently be a perfectly crystalline state, since if the packing density is maximum, the potential energy of the load application mechanism would be minimum. However, a loaded granular packing may be jammed at a looser, random state [22]. The perfectly crystalline state evidently has the lowest configurational entropy, for there is only one way for the system to manifest itself, and a random state will have a higher entropy, for there will be many microscopically indistinguishable ways the system can manifest itself while being subject to the same macroscopic conditions. We propose, therefore, that an effective way to describe the degree of randomness of a granular packing is the *retained configurational entropy*. Assuming that each random state can be characterized by the corresponding contact force distribution $P(f)$, the statistical entropy functional is defined as [18–20]

$$S=-k\int_0^\infty P(f)\ln[P(f)]df, \tag{1}$$

where k is a normalization constant analogous to the Boltzmann constant.

B. Equilibrium condition for static granular packing

When a loaded granular packing settles to equilibrium, the energy U must attain a local minimum value, subject to the constraint imposed by the retained entropy in Eq. (1). The corresponding variation principle is equivalent to minimizing the functional

$$F=U-\theta S, \tag{2}$$

where θ is the Lagrange multiplier associated with the constraint in Eq. (1). Let $W(f)$ be the work done by a contact force f between two grains. For a granular packing with a force distribution $P(f)$, the energy functional will be

$$U=\int_0^\infty P(f)W(f)df. \tag{3}$$

To find the equilibrium distribution, U should then be minimized, subject to the constraint imposed by the retained entropy in Eq. (1), as well as the additional constraints

$$\int_0^\infty fP(f)df=\overline{f}=\text{constant} \quad \text{and} \quad \int_0^\infty P(f)df=1. \tag{4}$$

The result is

$$P(f)=A\exp\left[-\frac{1}{k\theta}[W(f)-\lambda f]\right], \tag{5}$$

where A and λ are normalization constants that make $P(f)$ satisfy Eq. (4).

1. 2D Hertzian contact

To illustrate the results, let us consider the simple case of a two-dimensional (2D) granular packing in which the contact forces are purely Hertzian. For an elastic contact between two parallel circular disks, the Hertzian force law is given by [23]

$$f=\frac{\pi E_r a^2}{4R^*}, \tag{6}$$

where a is the radius of the circular contact region, E_r is the reduced modulus, and R^* is the relative curvature defined as

$$\frac{1}{R^*}=\frac{1}{R_1}+\frac{1}{R_2},$$

R_1 and R_2 being the radii of the two contacting disks. The reduced modulus E_r is defined as

$$\frac{1}{E_r}=\frac{1-\nu_1^2}{E_1}+\frac{1-\nu_2^2}{E_2},$$

where ν_i and E_i $(i=1,2)$ are the Poisson's ratio and Young's modulus of the disks, respectively.

For the sake of simplicity, let us consider the case when the 2D granular packing has identical disks. Let R be the common radius and ν and E be the common elastic constants, $R^*=R/2$ and $E_r=E/2(1-\nu^2)$, and the Hertzian force law in Eq. (6) becomes $f=\pi E_r a^2/2R$. The work done by f is

$$W(f)=-\int_0^\infty f\frac{dr}{da}da,$$

where $r=2\sqrt{R^2-a^2}$ is the distance between the grain centers. $W(f)$ can be shown to be given by

$$W(f)=\frac{2\pi E_r}{3}\left[R^2-\left(\frac{Rf}{\pi E_r}+R^2\right)\sqrt{1-\frac{2f}{\pi E_r R}}\right]\approx\frac{2f^2}{3\pi E_r}, \tag{7}$$

where the simplification at the end is accurate when f/E_rR is small compared to unity. With Eq. (7), $P(f)$ in Eq. (5) would adopt a Gaussian form

$$P(f)=A\exp[-\kappa(\langle f\rangle-f_o)^2], \tag{8}$$

where $\langle f\rangle=f/\overline{f}$, $\overline{f}$ being the mean force, and $\kappa=(2\overline{f}^2/3\pi E_r)(1/k\theta)$ is an inverse and dimensionless measure of the Lagrange multiplier θ. For each κ, the normalization constants A and f_o can be calculated to make $P(f)$ satisfy Eq. (4), and the results are given in Table I.

2. 3D Hertzian contact

In 3D, the Hertzian force law is [23]

$$f=\frac{4E_r a^3}{3R^*}, \tag{9}$$

TABLE I. Normalization constants for 2D equilibrium distribution in Eq. (8).

κ	f_o	A	Entropy S	Energy U (units of $2\overline{f^2}/3\pi E_r$)
0.01	−48.0365	1.03023×10^{10}	0.999823	2.10601
0.1	−3.22845	2.39813	0.990447	1.77155
0.2	−0.841848	0.848929	0.973891	1.65815
0.3	−0.0843688	0.652012	0.955138	1.58230
0.4	0.275758	0.597287	0.935470	1.52576
0.5	0.481058	0.582599	0.915435	1.48106
0.6	0.611026	0.583967	0.895306	1.44436
0.7	0.69914	0.593048	0.875240	1.41343
0.8	0.761838	0.606237	0.855331	1.38684
0.9	0.808085	0.621752	0.835638	1.36364
1	0.843156	0.638622	0.816198	1.34316
2	0.968629	0.819483	0.638307	1.21863
3	0.991399	0.984671	0.489865	1.15807
4	0.997355	1.13109	0.366268	1.12236
5	0.999142	1.26256	0.262571	1.09914
6	0.999713	1.38253	0.174389	1.08319
7	0.999903	1.49284	0.098638	1.07133
8	0.999967	1.59582	0.0323445	1.06247
9	0.999988	1.69259	−0.0263644	1.05554
10	0.999996	1.78413	−0.0789714	1.05000

so that for a uniform granular packing, it becomes $f=8E_r a^3/3R$. $W(f)$ can be shown to be given by

$$W(f)=\frac{2E_r}{3R}\left[-a\sqrt{R^2-a^2}(3R^2+2a^2)+3R^4\tan^{-1}\left(\frac{a}{\sqrt{R^2-a^2}}\right)\right].$$

As $a/R\to 0$,

$$W(f)\approx\frac{16E_r}{15R^2}a^5=\frac{2}{5R}\left(\frac{3R}{8E_r}\right)^{2/3}f^{5/3}. \tag{10}$$

Substituting Eq. (10) into Eq. (5) yields the following form for $P(f)$:

$$P(f)=A\exp[-\kappa(\langle f\rangle^{5/3}-\lambda\langle f\rangle)], \tag{11}$$

where $\kappa=(2/5R)(3R/8E_r)^{2/3}\,\overline{f}^{5/3}(1/k\theta)$, and A and λ are normalization constants given in Table II. Figures 1 and 2 show the equilibrium $P(f)$ at different values of κ for 2D and 3D, respectively. It is perhaps interesting to see that the 3D results in Fig. 2 show practically little difference with the Gaussian forms for 2D shown in Fig. 1.

C. Analogy with thermodynamics

The functional F in Eq. (2) evidently resembles a free energy in the thermal sense. The Lagrange multiplier θ is analogous to the absolute temperature. $\theta=0$ means that minimization of F is equivalent to minimization of E, subject to the constraints in Eq. (4). The result is $W(f)+\lambda_1 f+\lambda_2=0$, where λ_1's are Lagrange multipliers determined from the two constraints in Eq. (4). This is simply an algebraic equation in f and the solution to it would give definite values of f instead of a distribution $P(f)$. In other words, minimization of the energy functional alone always yields the Kronecker delta function for $P(f)$ and not a distribution. This is the limiting case of the distributions in Figs. 1 and 2 as $\kappa\to\infty$, and corresponds to the perfect crystalline behavior in which all contact forces must have the same value. This case is the zero-temperature analog in the thermal situation. On the other hand, in the limit $\theta\to\infty$, the entropy functional alone is to be maximized. When this is done, the result is the Maxwell-Boltzmann distribution $P(f)=\exp(-f/\overline{f})$, and corresponds to the limiting case of $\kappa\to 0$ in Figs. 1 and 2. This case corresponds to infinite temperature in the thermal situation, and is also the special case considered by Bagi [19] and Evesque [20]. The range $\theta\in[0,\infty)$ therefore spans the entire spectrum from perfect crystallinity to complete randomness, or from zero to infinite ''mechanical temperature.'' The relationship between κ and S (and U) is also shown in Tables I and II. Here, it can be seen that as the ''mechanical temperature'' or $1/\kappa$ decreases, both the entropy and energy decrease, again in analogy with the thermal situation.

III. COMPUTER SIMULATION

A. Method of simulation

The 2D and 3D simulations were performed using the discrete element method to illustrate the concepts developed

TABLE II. Normalization constants for 3D equilibrium distribution in Eq. (11).

κ	λ	A	Entropy S	Energy U [units of $(2\overline{f}^{5/3}/5R)(3R/8E_r)^{2/3}$]
0.01	−97.5038	0.990098	0.999966	1.49769
0.1	−7.58609	0.910329	0.997393	1.44835
0.2	−2.65166	0.835727	0.991587	1.40900
0.3	−1.03582	0.771267	0.984020	1.37851
0.4	−0.244008	0.714411	0.975338	1.35360
0.5	0.220947	0.663589	0.965903	1.33257
0.6	0.524021	0.617730	0.955939	1.31441
0.7	0.735547	0.576058	0.945593	1.29847
0.8	0.890488	0.537983	0.934972	1.28429
0.9	1.00814	0.503040	0.924153	1.27155
1	1.10001	0.470857	0.913195	1.26000
2	1.47197	0.251574	0.802442	1.18318
3	1.56771	0.138202	0.697786	1.14062
4	1.60532	0.076447	0.602646	1.11321
5	1.62347	0.0422501	0.517210	1.09406
6	1.63353	0.0232564	0.440699	1.08015
7	1.63970	0.0127356	0.372198	1.06950
8	1.64383	0.00693731	0.310593	1.06126
9	1.64679	0.00375993	0.254903	1.05477
10	1.64901	0.00202857	0.20110	1.04936

so far. The main purpose of the simulation is to compare with the theoretical development above. For the elastic contact between two solids, there is strong coupling between the tangential (frictional) forces and the normal pressure [23], which renders analytical development of the work done $W(f)$ in Eq. (3) difficult. For this reason, only Hertzian contact forces were considered in the simulation. The frictionless assumption is certainly unrealistic for rough grains, but may nevertheless act as a limiting or ideal behavior for the smooth grain situation. The issue of friction should better be addressed in a separate effort.

The 2D simulations were performed on 11 112 grains, and the grain sizes distributed approximately uniformly throughout a range of $\pm 10\%$ of the mean value to prevent crystallization. The initial packing configuration was generated by allowing a collection of randomly positioned disks to fall under gravity in a 2D rectangular container. The resultant contact forces due to gravity were subsequently relaxed away

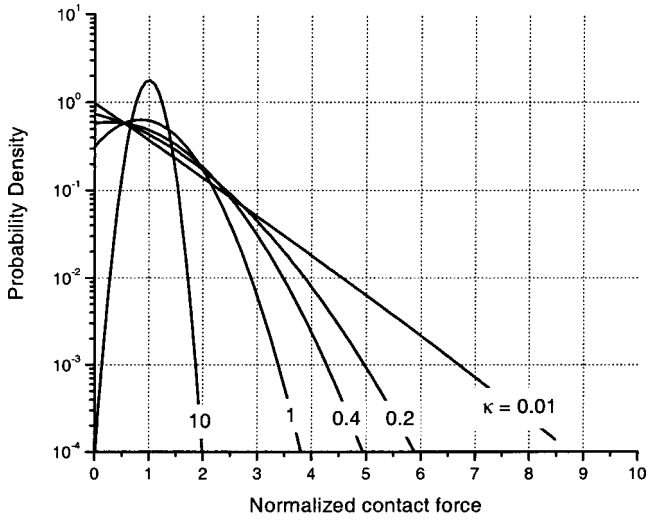

FIG. 1. 2D equilibrium force distribution at different ''mechanical'' temperatures. κ is an inverse measure of the mechanical temperature θ (see text).

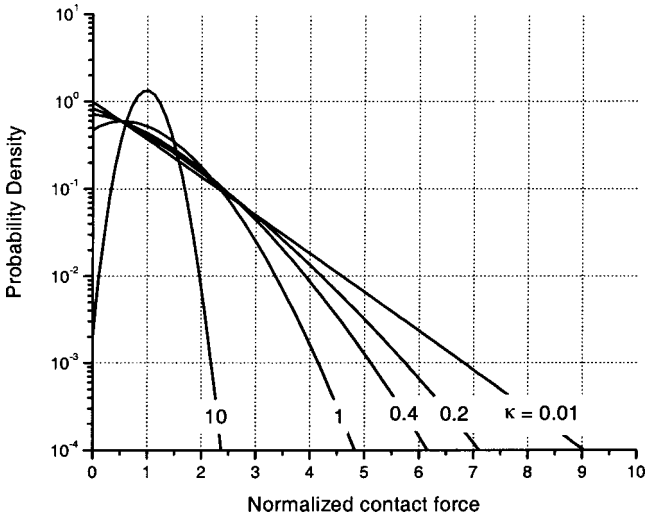

FIG. 2. 3D equilibrium force distribution at different ''mechanical'' temperatures. κ is an inverse measure of the mechanical temperature θ (see text).

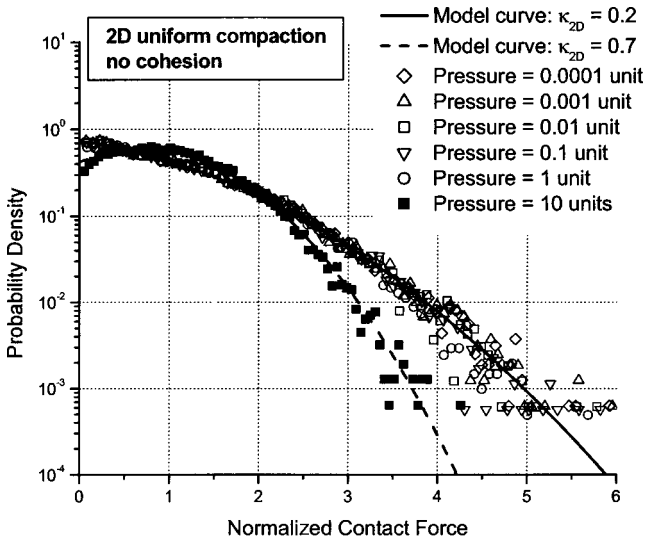

FIG. 3. Computer simulation results of contact force distribution in 2D under hydrostatic load. One unit of pressure $=5\times10^{-3}E$, E = Young's modulus.

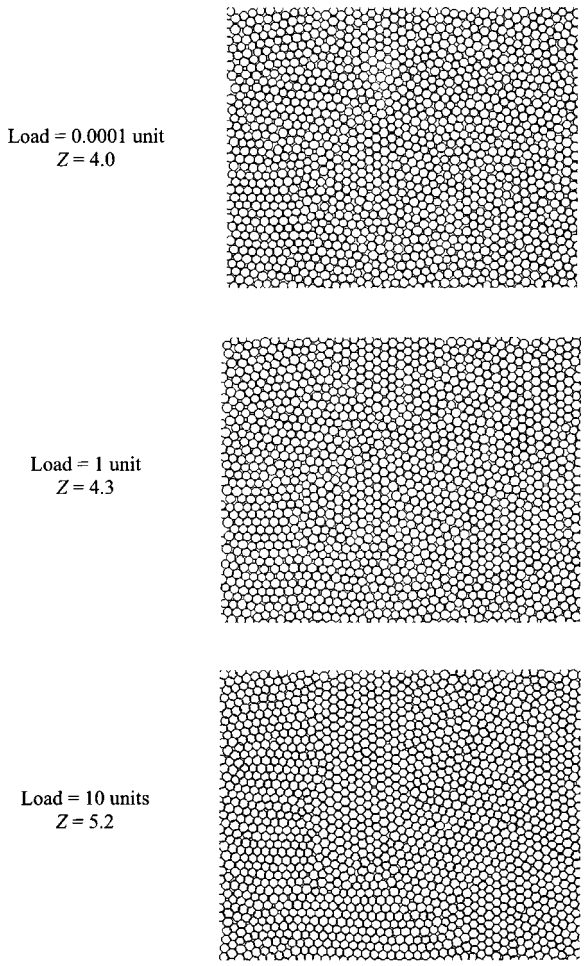

FIG. 4. 2D packings at different applied hydrostatic loads. Z is the average number of contacts per grain.

by switching off the gravity. This produced a strain-free initial packing configuration with density 0.83 and a rectangular dimension of $149\overline{d}\times70\overline{d}$ ($\overline{d}$ is the mean grain size). Compaction was performed by uniformly pressing the four sides of the rectangular packing by a given hydrostatic stress. The results presented below are from one initial configuration, but repeated calculation has also been done using another independently generated rectangular packing with a different aspect ratio of $102\overline{d}\times93\overline{d}$, but with the same initial packing density and a similar number of grains. The force distributions of the two packings were found to be identical, implying that the results are independent of the geometry of the packing as long as the initial packing density is the same. By virtue of the force law in Eq. (6), the unit of force (per unit length) in the simulation scales with the product $E_r\overline{d}$ and, as is obvious, the unit of stress scales with E_r or E (the Poisson's ratio of the grains was set to be 0.3). In the following results on 2D, 1 unit of pressure is defined as $5\times10^{-3}E$. If E is 200 GPa for example, 1 unit of pressure is equal to 1 GPa.

For the 3D simulations, 5×10^4 grains were simulated, and the grain size was uniform since it was observed that the structure did not crystallize easily. The initial structure was generated using a method similar to the 2D above. The density of the initial (stress-free) packing was 0.64. Compaction was also performed hydrostatically through applying the same compressive stress on all six sides of the rectangular packing. As for 2D, the unit of pressure in the 3D simulation scales with E_r. The results for 3D below are quoted directly in terms of GPa where the Young's modulus was assumed to be 200 GPa, and Poisson's ratio 0.3.

B. Results

Figure 3 shows the simulated results for 2D. It can be seen that the normalized force distribution is invariant with respect to the applied hydrostatic load over a four-order-of-magnitude change of load up to about 1 unit. The probability curves from 0.0001 to 1 unit of load can be fitted accurately by Eq. (8) with $\kappa=0.2$. The curve at 10 units of load can be fitted accurately by $\kappa=0.7$. A good fit in both cases indicates the validity of the theory above, namely, the equilibrium distribution corresponds to minimization of energy while entropy is held constant. The fitted results also indicate that κ is constant over a four-order-of-magnitude change in the applied load up to about 1 unit, but starts to decrease when the load becomes larger.

The decrease in the parameter κ beyond 1 unit of load is accompanied by an observed drastic change in the average number of contacts per grain, which remained roughly constant at the rigid-grain limit [24] of 4 when the load was smaller than about 1 unit, but increased to 5.2 when the load was 10 units. The higher coordination at large loads corresponds to a more regular arrangement or increased degree of crystallinity of the packing. Figure 4 shows the packing configurations at different applied hydrostatic loads. It can be seen that the packing at the slightest load of 0.0001 unit is rather loose, and many grains evidently make four contacts with neighbors, i.e., the structure is within the rigid-grain regime [24]. The packing at 1 unit of load is denser, but the degree of crystallinity is still not high, with the majority of

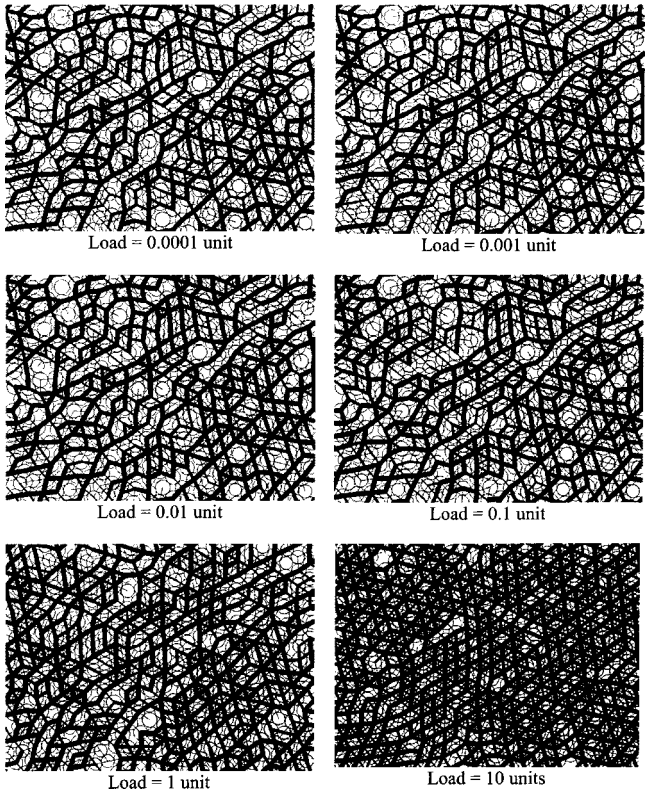

FIG. 5. Force networks in 2D packings at different applied hydrostatic loads. The width of the lines denotes the contact force magnitude. In each force pattern, the linewidths are normalized by a factor proportional to the overall load applied. The same central region of the granular packing is shown for all force patterns.

grains not in the closely packed condition of making six contacts with neighbors. When the load is increased to 10 units, the packing exhibits a polycrystalline morphology with closely packed domains separated by clear boundaries. The coordination number within each domain is usually 6. To conclude, the packing morphology changes very mildly from 0.0001 to 1 unit of load, but undergoes a significant change from 1 to 10 units of load. This marks a structural transition at about 1 unit of load, which can be identified as polycrystallization.

The structural transition past 1 unit of load can be visualized more clearly by the contact force networks shown in Fig. 5. Here, the width of the line joining each pair of contacting disks is set to be proportional to the contact force between the disks and inversely proportional to the overall applied stress on the granular packing. The same central region of the granular packing is shown for comparison purposes. It can be seen that the force network remains practically frozen from 0.0001 to about 0.1 unit of load, implying that in the low-pressure regime, the local contact forces are simply proportional to the applied load, without significant variations in the spatial distribution. However, at 1 unit of load, the force network starts to undergo observable changes and at 10 units of load, the pattern appears remarkably different, exhibiting a much more homogeneous force distribution, as suggested by Fig. 3.

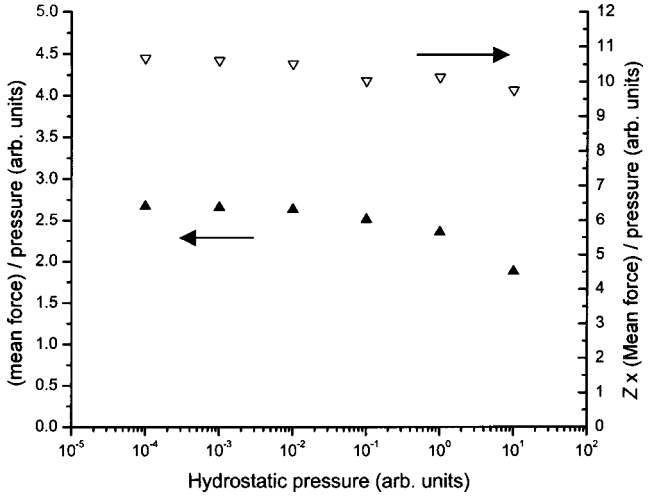

FIG. 6. Variation of mean force $\overline{f}$ observed in 2D simulations at different hydrostatic pressures.

The mean contact force $\overline{f}$ from the 2D simulations is also found to be proportional to the applied hydrostatic pressure in the rigid-grain regime where the average coordination number Z is 4 and the fitted κ_{2D} is 0.2, except at the largest simulated load of 10 units, where $\overline{f}$ is observed to be 30% smaller than what the proportionality relation predicts, as shown in the lower plot in Fig. 6. The 30% reduction in $\overline{f}$ at 10 units of load is accompanied by a corresponding increase in Z by 30% from 4 to 5.2 as noted before, i.e., the quantity $Z\overline{f}$ is found to be proportional to the applied pressure, as indicated in the upper plot in Fig. 6. In fact, one may expect $Z\overline{f}=\sigma\pi d$, a condition when the applied hydrostatic pressure σ is balanced on the individual grain level. The proportionality constant between $Z\overline{f}$ and σ observed in the upper plot in Fig. 6 is indeed very close to the value πd used in the simulations, where the mean grain diameter d was fixed at three length units.

The 3D simulation results, shown in Figs. 7 and 8, are

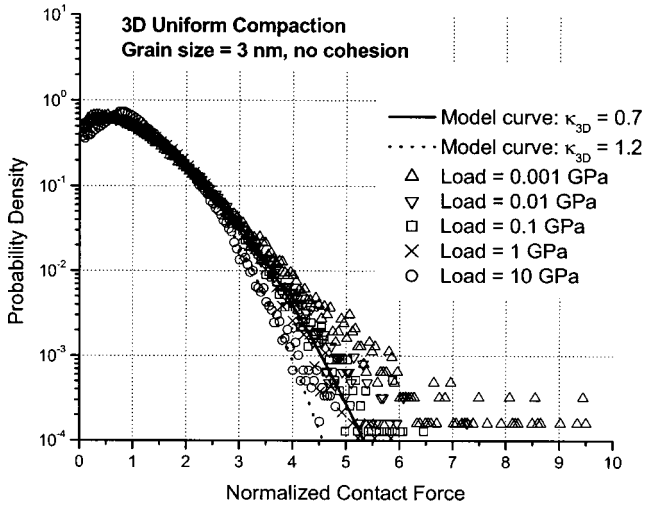

FIG. 7. Computer simulation results of contact force distribution in 3D under hydrostatic load.

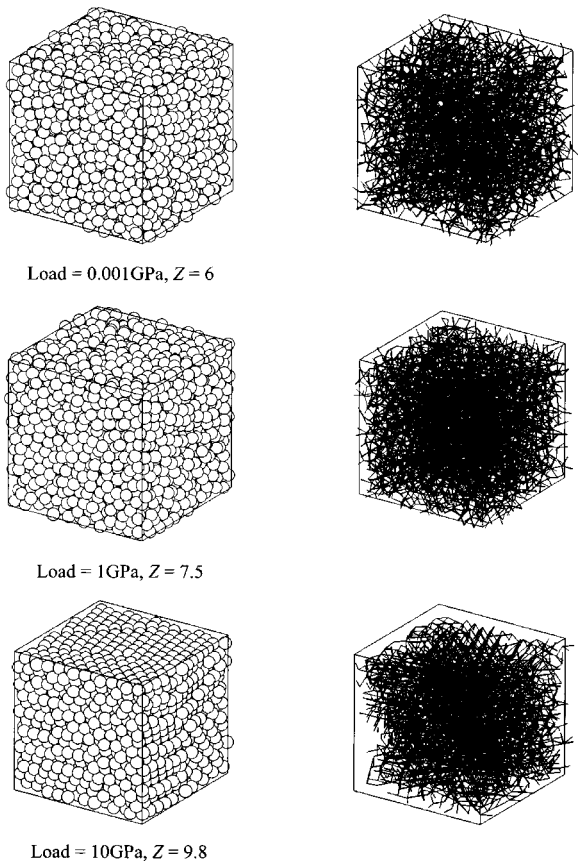

FIG. 8. (Left) 3D packings at different applied hydrostatic loads. (Right) Force networks at different loads. The width of the lines denotes the contact force magnitude. In each force pattern, the linewidths are normalized by a factor proportional to the overall load applied. The same central region of the granular packing is shown for all force patterns.

similar. In Fig. 7, it can be seen that the force distributions under applied pressure from 0.001 to 1 GPa can all be accurately fitted by Eq. (11) with the κ_{3D} parameter chosen to be 0.7. Within this load range, the average coordination number Z of the packing rises mildly from the rigid-grain limit [24] of 6 at 0.001 GPa to 7.5 at 1 GPa, as shown in Fig. 8. The packing morphologies and force networks shown in Fig. 8 have indeed undergone only very mild changes from 0.001 GPa to 1 GPa. However, at 10 GPa, polycrystallization into close-packed domains occurs, and this is accompanied by an abrupt change in the force network pattern in Fig. 8, in which hard contacts can be seen to occur along closely packed directions locally. Accompanying this change at 10 GPa is the drastic rise of Z to 9.8, and an increase of the fitted κ_{3D} value to 1.2, as shown in Fig. 7. Higher compaction loads were not simulated because the particle deformation calculated from the observed mean force at the largest load of 10 GPa is already 8.8%, and it is doubtful whether the type of the force law assumed in the simulation would still be valid at such a high elastic deformation. To investigate the effect on the force distribution of changing the structure by a larger extent, other means of densification, such as mechanical vibration, may be used, but this is beyond the scope of the present investigation.

IV. DISCUSSION

The most significant result from the present investigation is that the force distribution in a static, granular packing with uniform grain size and Hertzian contact force law is predicted to be Gaussian in 2D [Eq. (8)] and nearly Gaussian in 3D [Eq. (11), Fig. 2]. Moreover, the exponential MB distribution is recovered as a limiting case of the Gaussian (or nearly Gaussian) distribution, in the limit as the mechanical temperature, or the system's randomness, tends to infinity. The predicted Gaussian or the limiting MB distribution are in agreement with the simulated results in the literature [4,5,7,8]. In particular, O'Hern *et al.* [8] have observed that the simulated force distributions for a harmonic and a Hertzian force law are both Gaussian. Their Hertzian results are what is predicted in the present study. For a harmonic force law, W scales with f^2, and this is fortuitously the case considered in the simplification step in Eq. (7) for a 2D Hertzian contact. The distribution for a harmonic force law should, therefore, be given by the same Gaussian form as in Eq. (8), and O'Hern *et al.*'s observation can, therefore, be explained. Most experimental force distributions, however, exhibit a peak near the mean force value with an exponential tail in the large force regime [1–3,6]. As suggested by O'Hern *et al.* [8], the discrepancy between such a behavior and the Gaussian form is likely to be due to friction in the experimental situation.

Another interesting finding from the present investigation is that the simulated force distributions in Fig. 3 for 2D and in Fig. 7 for 3D are invariant within the rigid-grain limit, and a structural transition at higher loads results in sharper distributions. This appears to be different from the simulated results obtained by Makse, Johnson, and Schwartz [4], who have observed that the force distribution undergoes a gradual transition from the MB behavior for small pressures to a Gaussian form for larger pressures. It should however, be noted that the simulation conditions in the two studies are very different. In the study of Makse, Johnson, and Schwartz, friction was included, and the grain size varied by $\pm 5\%$, while in the present 3D simulations, the grains have uniform size and are frictionless. The grain size was chosen to be uniform in the present simulations because the objective was to compare with the theoretical development, and in the latter, it was difficult to deal with a spread grain size distribution as well as friction in the derivation of the work done terms in Eqs. (7) and (10). With friction and a spread size distribution. Makse, Johnson, and Schwartz were able to obtain very loose but jammed configurations with coordination number as low as 4, as compared to the rigid-grain limit of 6 in the frictionless case. It is, however, interesting to see that the family of the force distributions observed by Makse, Johnson, and Schwartz during the transition from the MB to the Gaussian form as pressure and coordination increase seems to correspond well to the curves in Fig. 2, as κ increases (cf. Fig. 2 of Makse, Johnson, and Schwartz [4] and Fig. 2 of the present study). This reinforces the idea that the parameter κ is a structure sensitive parameter, as discussed above, but of course it must be remembered that the appli-

cability of the present results to the situation with friction is strictly speaking uncertain.

In the present study, the lowest coordination observed is 6 in 3D, in agreement with the observation of Makse, Johnson, and Schwartz who have also simulated the frictionless case. However, the frictionless results of Makse, Johnson, and Schwartz do not indicate an abrupt rise in coordination number at a high pressure, as shown in Fig. 8 (see Fig. 1 of Ref. [4]). The maximum coordination number obtained by Makse, Johnson, and Schwartz is below 8, which indicates no crystallization. The absence of polycrystallization in the study of Makse Johnson, and Schwartz is probably due to the lower pressure and the spread grain size used. The maximum pressure used by Makse, Johnson, and Schwartz was $1.4 \times 10^{-3}E$, where E is Young's modulus (data from Ref. [4]: maximum pressure 100 MPa Poisson's ratio$=0.2$, shear modulus$=29$ GPa,) while the maximum pressure used in the present study is $0.05E$ (maximum pressure 10 GPa, $E = 200$ GPa). Although the high pressure results in the present study may be unrealistic, since the force law assumed may no longer be valid at pressures as high as $0.05E$, the procedure here nevertheless yields a polycrystallized structure, as shown in Fig. 8, which could be used to illustrate that a different structure has a different value of κ, as shown in Fig. 7. The key point is that the polycrystallized structure at 10 GPa in Fig. 8 could be unloaded carefully to keep the coordination, and if reloaded to a lower and hence realistic pressure, it will exhibit a different κ as compared to a random structure.

As mentioned before, the Lagrange multiplier θ in Eq. (2) may be viewed as an analog of the thermal temperature controlling the mixity of strain energy and entropy contributions in the free-energy F. In 2D, from Eq. (8),

$$k\theta = \frac{2\overline{f^2}}{3\pi E_r}\frac{1}{\kappa_{2D}}. \tag{12}$$

We have seen in Fig. 6 that $Z\overline{f}$ is proportional to the applied pressure σ, and therefore, from Eq. (12), $\theta \propto \sigma^2/Z^2\kappa_{2D}$. The θ calculated from Eq. (12) is plotted against the applied hydrostatic load in Fig. 9, where it can be seen that θ is indeed proportional to the square of the applied pressure in the rigid-grain regime of $Z=4$, and when the rigid-grain limit is exceeded ($Z>4$), departure from the quadratic behavior occurs. The results in Fig. 3 indicate clearly that κ_{2D} is constant with respect to load within the rigid-grain limit. The fact that the packing configuration and the force network are both invariant within this regime, as shown in Figs. 4 and 5, indicates that κ_{2D} depends on the structure of the packing but not on the load, as long as the load is not large enough to cause structural changes. This observation allows one to decompose Eq. (12) into

$$\theta = \overline{f^2} \quad (\text{for } 2\text{D}) \tag{13}$$

and

$$k = \frac{2}{3\pi E_r \kappa_{2D}} \quad (\text{for } 2\text{D}). \tag{14}$$

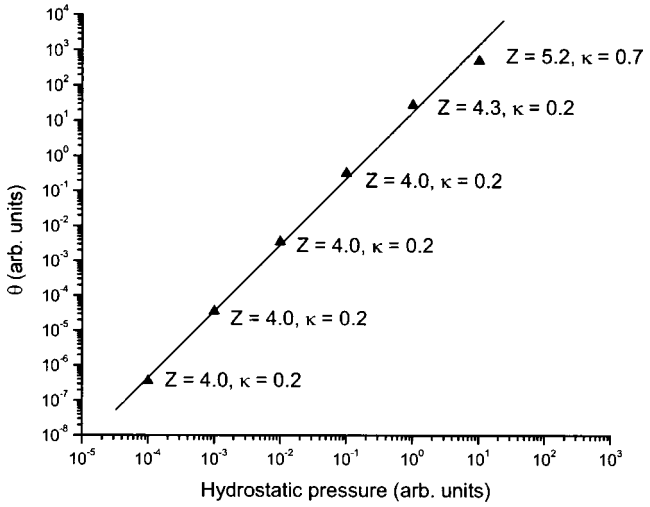

FIG. 9. θ vs applied hydrostatic pressure in 2D simulations. The average coordination number Z is 4 in the rigid-grain regime, and increases beyond 4 as the grains are compressed when the pressure is very high. θ is calculated according to Eq. (12) using the fitted κ in Fig. 3 and the mean force $\overline{f}$ observed in the simulations.

With such a decomposition, k can be identified as a structure-sensitive term—it carriers the dependence on structure through κ_{2D}, and on material through E_r. θ carries the dependence on the load through $\overline{f}$. Similarly, for 3D, we can write [cf. Eq. (11)]

$$\theta = \overline{f}^{5/3} \quad (\text{for } 3\text{D}) \tag{15}$$

and

$$k = \frac{2}{5R\kappa_{3D}}\left(\frac{3R}{8E_r}\right)^{2/3} \quad (\text{for } 3\text{D}). \tag{16}$$

At constant structure, the increasing relationship between θ and $\overline{f}$ is analogous to the thermal situation, e.g., in an ideal gas, where the absolute temperature is proportional to the mean internal energy.

It may be of interest to state the dependence of the conclusions so far on physical parameters such as elastic modulus and grain size. The effects of the modulus and grain size can, in fact, be deduced easily from the force laws used in Eqs. (6) and (9). In the Hertzian force law for 2D or 3D, the contact force between two grains is proportional to the reduced modulus E_r. Hence, if the modulus is, say, doubled, the load has to be doubled to maintain the same deformation at the contact. Thus, the deformation on doubling the modulus but keeping the load unchanged is the same as that on halving the load but maintaining the modulus. Within the rigid-grain limit, the κ value is independent of load, and so changing the modulus would have no effect on the κ value. The κ value, however, would decrease with increasing E_r according to Eq. (14) or Eq. (16). The effect of grain size can also be deduced in a similar way. In 2D, for example, the particle deformation (strain) is measured by $(a/R)^2$ [see Eq. (6)]. Therefore, if R is doubled, the force f in Eq. (6) needs to be doubled to maintain the deformation. However, doubling

both the length scale and the force implies that the applied pressure is unchanged in 2D. Hence, changing the grain size can have no effect on the deformation if the applied pressure is unchanged. The same conclusion can also be drawn for 3D using Eq. (9). Therefore, κ is also unaffected by changing the grain size. According to Eq. (14), κ for 2D is also independent of the grain size, but Eq. (16) suggests that κ for 3D decreases with increasing grain size.

The current mechanical analog of temperature θ is similar in nature to other effective temperatures proposed by previous researchers for athermal but fluctuating systems [17–21]. Edwards [18] has proposed a quantity known as compactivity for granular packings, and this is also an analog to temperature. Edwards' treatment deals with the problem of filling a volume V by a granular powder, and statistical physical concepts were introduced by drawing analogy between volume and energy. Edwards' expression for the free-energy analog is [18]

$$F = V - X(\partial F/\partial X), \tag{17}$$

where X is the compactivity analogous to θ in our present treatment [cf. Eq. (2)]. Energy itself did not come in as a direct focus for consideration in Edwards' treatment. However, the problem of filling space itself clearly has much relevance to energy minimization. For the case of packing a powder under gravity, for example, gravitational potential energy should attain a local minimum when equilibrium is reached, and for the case of compaction by a loaded piston, the work done on the piston should also reach a minimum. The two temperatures X and θ are, therefore, clearly related, as for the perfectly crystalline system, both the compactivity and the mechanical temperature θ would be zero, and for the maximally disordered system (i.e., that having the Maxwell-Boltzmann force distribution), both the compactivity and θ would be very large. The current mechanical temperature θ is also closely related to the dynamic granular temperature proposed by Jaeger, Liu, and Nagel [17]. The temperature of Jaeger, Liu, and Nagel measures the extent of the fluctuations available to cause avalanches in a dynamic grain pile. It should, therefore, be closely related to Edwards' compactivity X or the current mechanical temperature θ, i.e., a densely packed powder has small compactivity and is also more difficult to exhibit avalanches. A detailed analysis on the mathematical relationship between X and θ would require the mean energy U to be expressed as a function of grain volume. This may not be done analytically but may be performed numerically. Such an analysis is beyond the scope of the present work and may be pursued as a future exercise. Lastly, Ono *et al.* [21] have also investigated a similar effective temperature as θ here, namely, the reciprocal of the rate of change of the entropy with respective to energy, dS/dU [cf. Eq. (2)]. Ono *et al.* [21] have shown that, for a sheared elastic foam, such a definition of temperature agrees with other definitions of temperatures concerning fluctuations in system properties (pressure, shear stress, energy), as well as viscosity. Ono *et al.* calculated dS/dU by randomly generating foam structures and considering the probability distribution of the energies of these structures. dS/dU is then obtained as the slope of the log(probability) vs energy plot at a certain energy. It is clear that such an approach is applicable to a dynamic system only, since a randomly generated configuration is usually not in mechanical equilibrium. Therefore, the present θ has nothing to do with this effective temperature calculated by Ono *et al.*

V. CONCLUSIONS

In structurally random materials, such as a granular packing, the internal force distribution due to external loading is not uniform. The internal force distribution enables the definition of an energy as well as an entropy functional. It is proposed here to use the retained entropy as a numerical measure of the degree of randomness. Minimization of the energy functional subject to the constraint imposed by the retained entropy yields force distributions in excellent agreement with computer simulation results. The constrained variational principle of energy minimization is also equivalent to that of minimization of a free-energy functional consisting of a mixture of energy and entropy. The mixity between the energy and entropy is controlled by a parameter known as the ''mechanical temperature.'' At constant structure, the mechanical temperature is found to increase with the applied loading or the mean value of the intergranular contact forces.

ACKNOWLEDGMENT

This work was supported by a research grant from the University Research Committee of the University of Hong Kong (Project No. 10204222.16180.14500.323.01).

[1] C. H. Liu *et al.*, Science **269**, 513 (1995).
[2] F. Radjai *et al.*, Phys. Rev. Lett. **77**, 274 (1996).
[3] D. M. Mueth, H. M. Jaeger, and S. R. Nagel, Phys. Rev. E **57**, 3164 (1998).
[4] N. A. Makse, D. L. Johnson, and L. M. Schwartz, Phys. Rev. Lett. **84**, 4160 (2000).
[5] M. L. Nguyen and S. N. Coppersmith, Phys. Rev. E **62**, 5248 (2000).
[6] J. M. Erikson *et al.*, Phys. Rev. E **66**, 040301(R) (2002).
[7] C. S. O'Hern *et al.*, Phys. Rev. Lett. **86**, 111 (2001).
[8] C. S. O'Hern *et al.*, Phys. Rev. Lett. **88**, 075507 (2002).
[9] S. N. Coppersmith *et al.*, Phys. Rev. E **53**, 4673 (1996).
[10] J. E. S. Socolar, Phys. Rev. E **57**, 3204 (1998).
[11] P. Claudin *et al.*, Phys. Rev. E **57**, 4441 (1998).
[12] M. L. Nguyen and S. N. Coppersmith, Phys. Rev. E **59**, 5870 (1999).
[13] O. Narayan, Phys. Rev. E **63**, 010301(R) (2000).
[14] J. Rajchenbach, Phys. Rev. E **63**, 041301 (2001).
[15] M. Lewandowska, H. Mathur, and Y. Yu, Phys. Rev. E **64**, 026107 (2001).

[16] D. L. Blair *et al.*, Phys. Rev. E **63**, 041304 (2001).
[17] H. M. Jaeger, C. Liu, and S. R. Nagel, Phys. Rev. Lett. **62**, 40 (1988).
[18] S. F. Edwards, in *Granular Matter—An Interdisciplinary Approach*, edited by A. Mehta (Springer-Verlag, New York, 1994), Chap. 4.
[19] K. Bagi, in *Powders and Grains 97*, edited by R. P. Behringer and J. T. Jenkins (A.A. Balkema, Rotterdam, The Netherlands 1997), p. 251.
[20] P. Evesque, in *Powders and Grains 2001*, edited by Y. Kishino (A.A. Balkema, Lisse, The Netherlands, 2001), p. 153.
[21] I. K. Ono *et al.*, Phys. Rev. Lett. **89**, 095703 (2002).
[22] *Jamming and Rheology*, edited by A. J. Liu and S. R. Nagel (Taylor and Francis, New York, 2001).
[23] K. L. Johnson, *Contact Mechanics* (Cambridge University Press, Cambridge, 1985), p. 101.
[24] C. F. Moukarzel, in *Rigidity Theory and Applications*, edited by M. F. Thorpe and P. M. Duxbury (Kluwer Academic/Plenum, New York, 1999), p. 125.